

Supporting Information: Pearl-Necklace-Like Local Ordering Drives Polypeptide Collapse

Suman Majumder,^{*,†} Ulrich H.E. Hansmann,^{*,‡} and Wolfhard Janke^{*,†}

[†]*Institut für Theoretische Physik, Universität Leipzig, IPF 231101, 04081 Leipzig, Germany, and*

[‡]*Department of Chemistry and Biochemistry, University of Oklahoma, Norman, Oklahoma 73019,*

United States

E-mail: suman.majumder@itp.uni-leipzig.de; uhansmann@ou.edu; wolfhard.janke@itp.uni-leipzig.de

Here we present supporting information including figures we left out in the main manuscript for brevity. This includes i) the contact maps for different independent simulations and their variation with respect to the other chain lengths that are not presented in the main manuscript and ii) the contact probabilities for $(\text{Gly})_{100}$ and $(\text{Gly})_{150}$.

Contact maps for $(\text{Gly})_{20}$

In Figure 1a of the main manuscript, we have presented the time evolution of the residue contact maps for $(\text{Gly})_{20}$ during its collapse. There they are from only one simulation out of the total 50 independent simulations which we ran. Here, in Figure 1 we present such contact maps at four different times (same as presented in the main manuscript) from four other independent simulations, each of which were performed starting from a different initial configuration or replica. The sequence of events that can be observed is the same

*To whom correspondence should be addressed

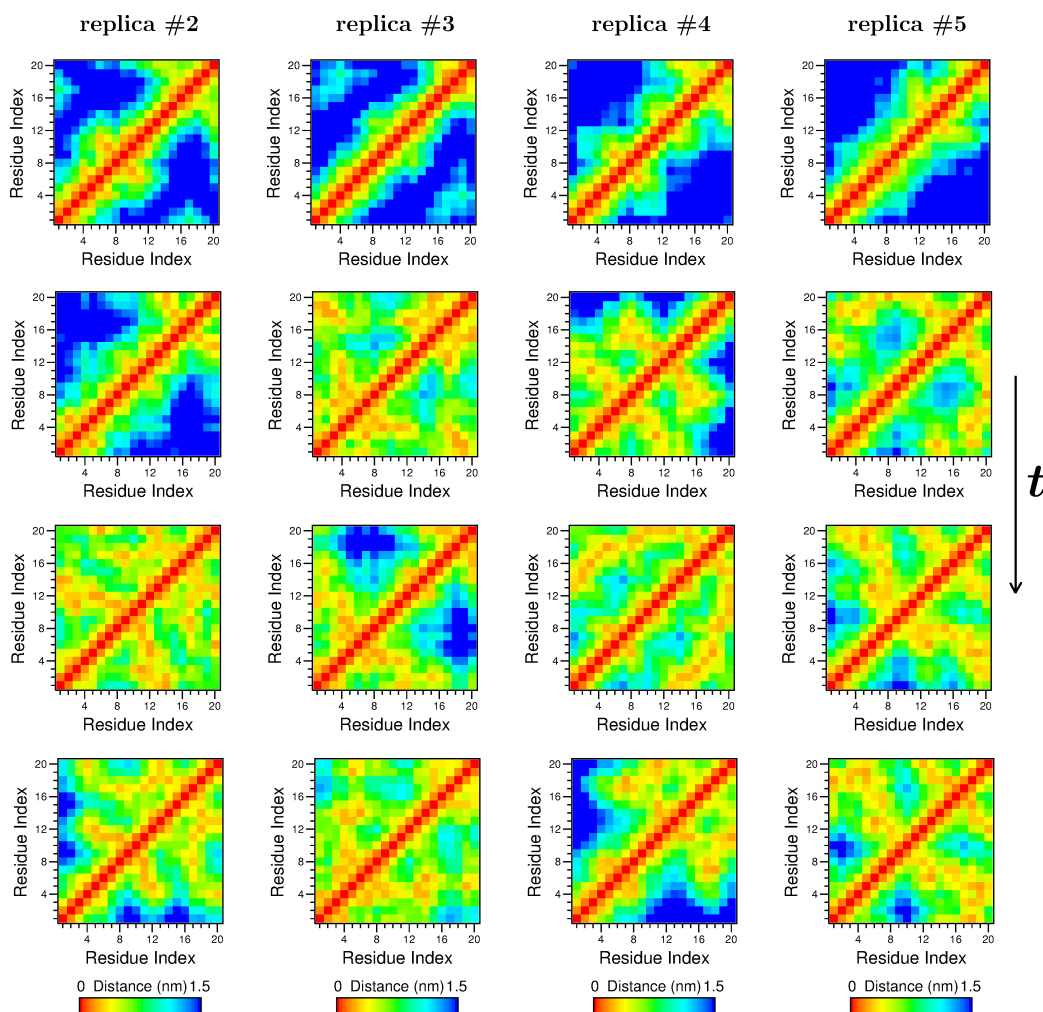


Figure 1: Residue contact maps at four different times, i.e., 0 ns, 2 ns, 5 ns, and 10 ns, for the collapse of $(\text{Gly})_{20}$. Results from four randomly picked simulations are shown. Note that these simulations correspond to the replicas that are presented in Figure 1b of the main text.

as the one presented in the main manuscript, i.e., one does not notice any special feature during the collapse.

Contact maps for $(\text{Gly})_{200}$

The residue contact maps during the collapse of $(\text{Gly})_{200}$ are presented in Figure 2a of the main manuscript. Those are for only one independent simulation. Here, in Figure 2 we present such contact maps from four other independent simulations. The sequence of

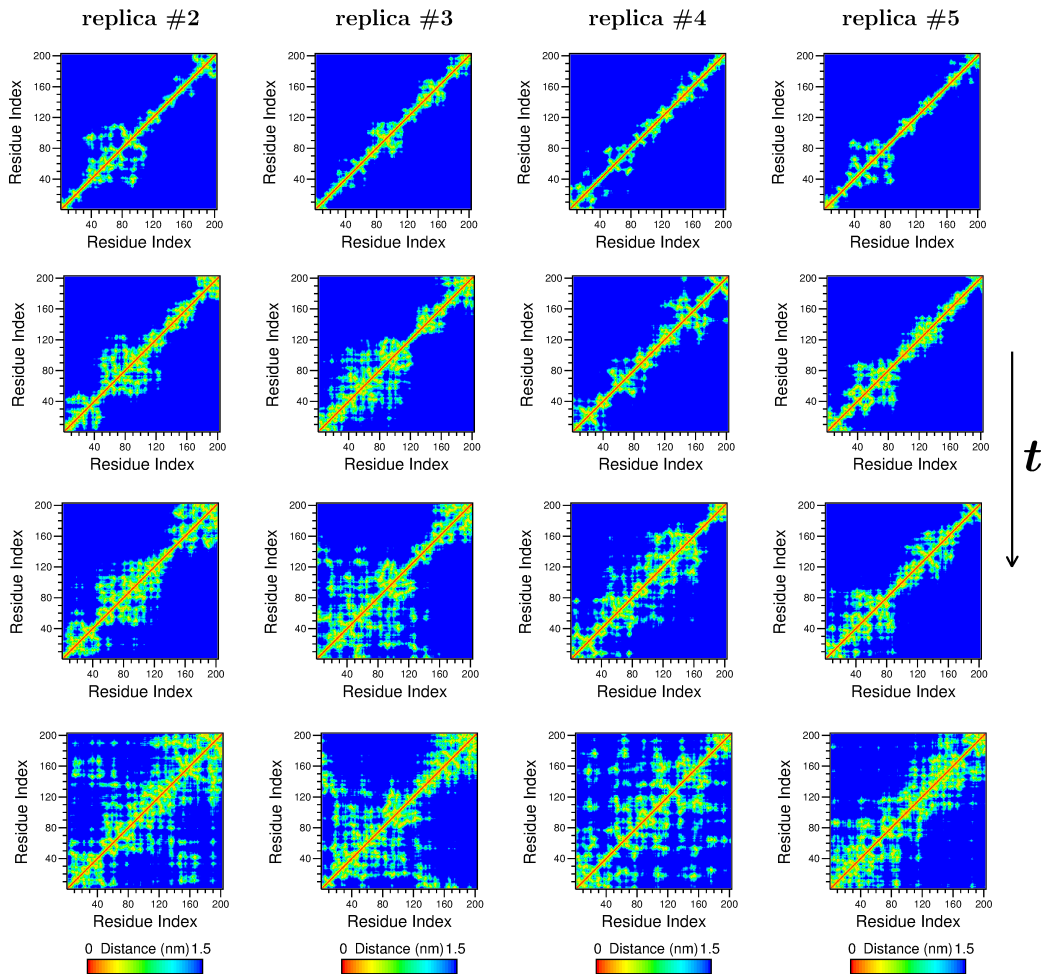


Figure 2: Residue contact maps at four different times, i.e., 0 ns, 2 ns, 5 ns, and 20 ns, for the collapse of $(\text{Gly})_{200}$. Results from four randomly picked simulations are shown. Note that these simulations correspond to the replicas that are presented in Figure 2b of the main text.

events, i.e., the formation of local ordering or pearl-necklace formation was observed in all the simulations. The corresponding variations of the squared radius of gyration R_g^2 are shown in Figure 2b of the main text.

Contact maps for different chain lengths

In this section we present the variation of the residue contact maps with respect to chain lengths. In the main manuscript we have presented results only for the shortest ($N = 20$)

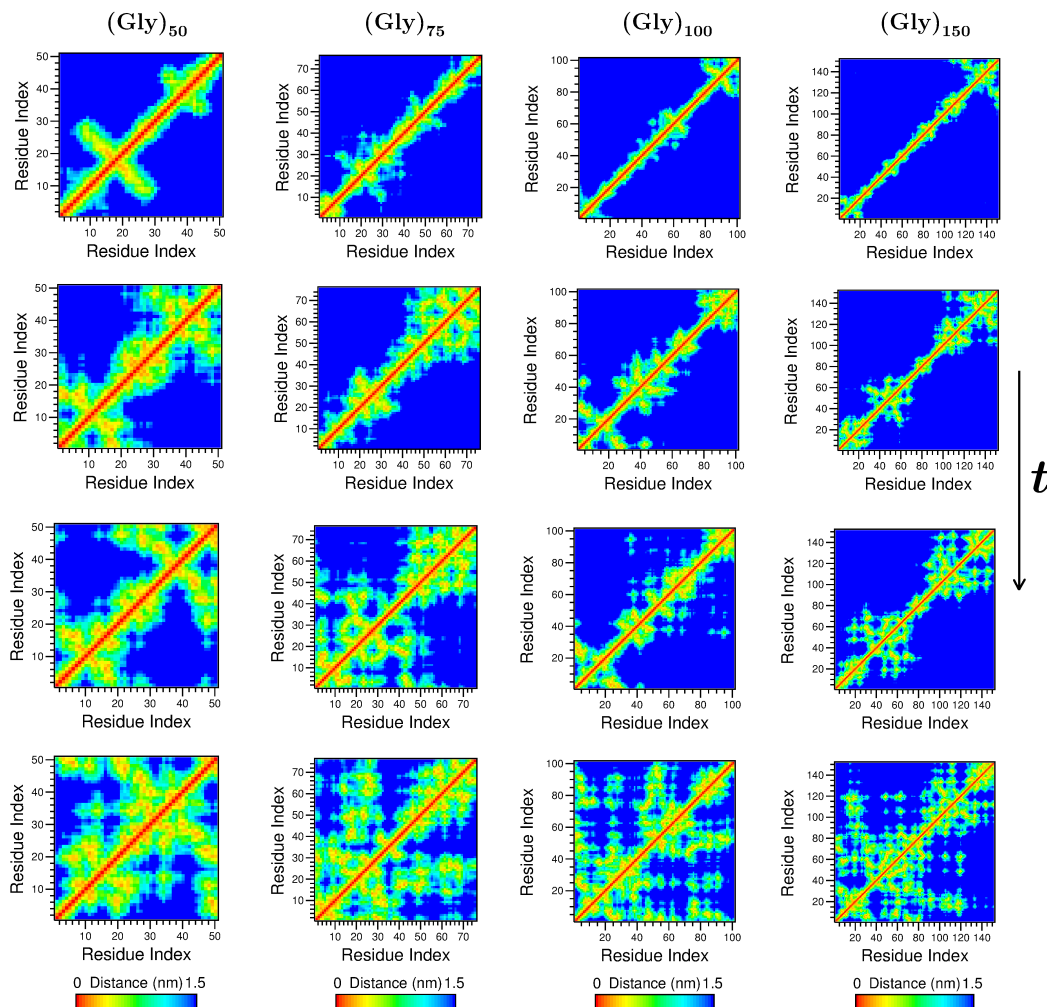


Figure 3: Residue contact maps at four different times, i.e., 0 ns, 2 ns, 5 ns, and 15 ns, for the collapse of $(\text{Gly})_N$ with four different N , as indicated. These results are from one simulation chosen randomly out of the several independent simulations ran for each case.

and the longest ($N = 200$) chains. Here, in Figure 3 we show the results for four other chain lengths, as indicated. Here also, for $N \geq 100$ the formation of local ordering, as described in the main text for $N = 200$, is clearly visible (discrete patches around the diagonal).

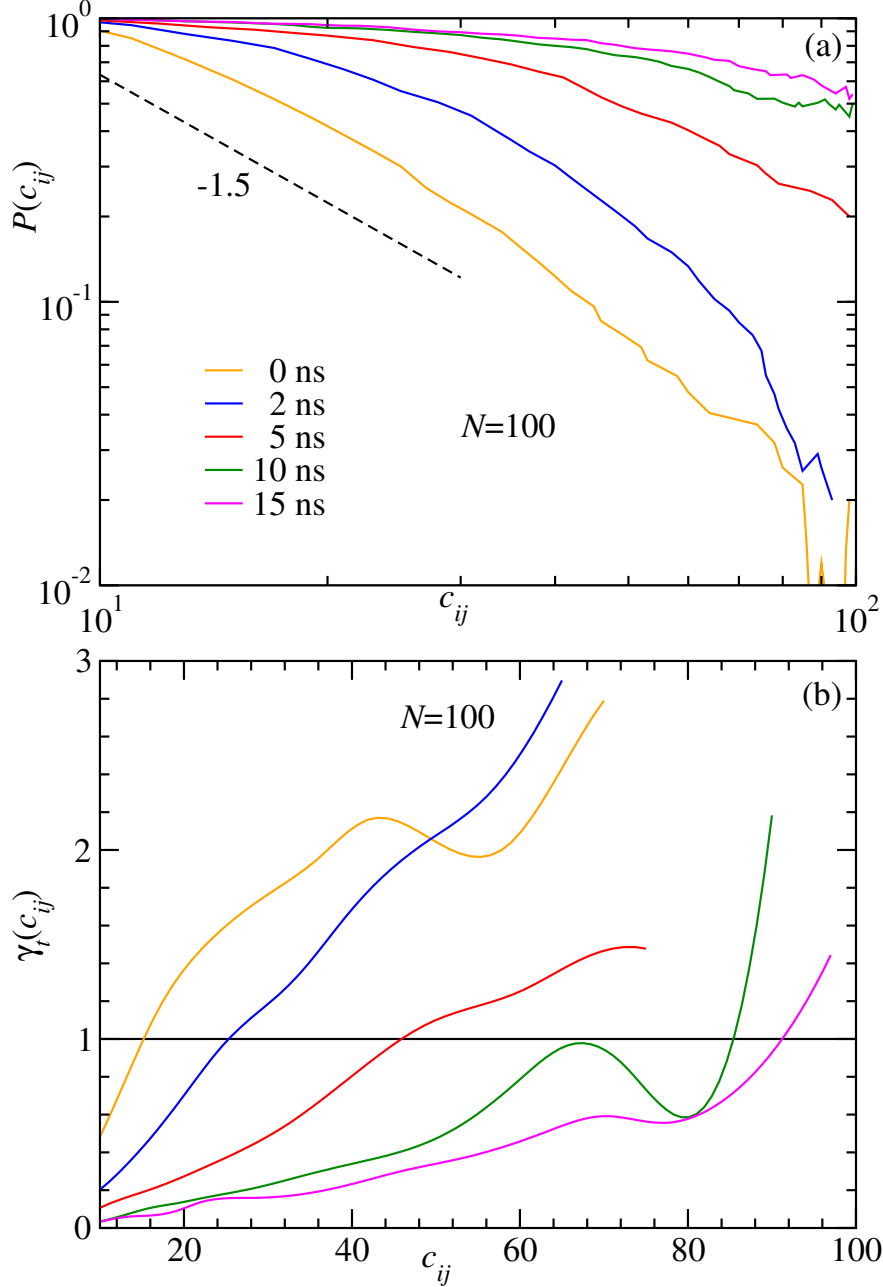


Figure 4: (a) Contact probability $P(c_{ij})$ calculated using the cut-off $r_c = 2.5$ nm, as a function of the distance c_{ij} along the chain, at five different times during collapse of $(\text{Gly})_{100}$. The dashed line there represents a power-law decay $P(c_{ij}) \sim c_{ij}^{-\gamma}$ with an exponent $\gamma = 1.5$ as expected in a good solvent. (b) The discrete slope γ_t obtained from Eq. (1) as a function of c_{ij} for the times presented in (a). The solid line is for $\gamma_t = 1$.

Contact probabilities for different chain lengths

For monitoring the growth of the pearl-necklace like clusters during the collapse, we have calculated the contact probability $P(c_{ij})$ as a function of the contour distance $c_{ij} = |i - j|$

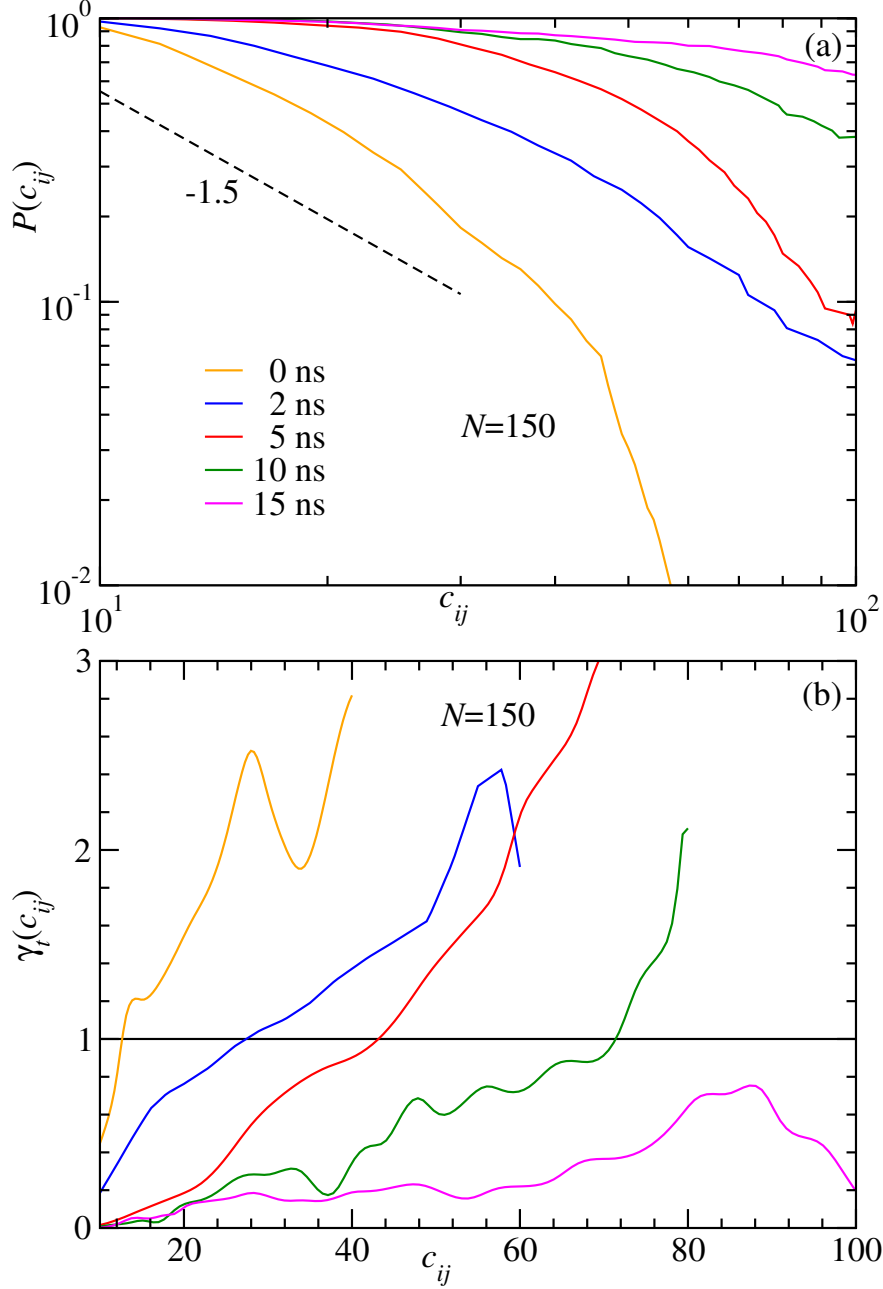


Figure 5: (a) Contact probability $P(c_{ij})$ calculated using the cut-off $r_c = 2.5$ nm, as a function of the distance c_{ij} along the chain, at five different times during collapse of $(\text{Gly})_{150}$. The dashed line there represents a power-law decay $P(c_{ij}) \sim c_{ij}^{-\gamma}$ with an exponent $\gamma = 1.5$ as expected in a good solvent. (b) The discrete slope γ_t obtained from Eq. (1) as a function of c_{ij} for the times presented in (a). The solid line is for $\gamma_t = 1$.

between any two $\text{C}\alpha$ -atoms at the i -th and j -th position along the chain. Two $\text{C}\alpha$ -atoms are said to have a contact if they are within a cut-off distance $r_c = 2.5$ nm.

In Figure 5a of the main text, we have presented the corresponding results for (Gly)₂₀₀. Here, in Figures 4a and 5a we present the analogous results for (Gly)₁₀₀ and (Gly)₁₅₀, respectively. Here also, as described in the main text one can observe that as time progresses $P(c_{ij})$ decays slower and slower along with a change in slope. This fact, or crossover in the slope is used to calculate the relevant length scale, i.e., mean pearl or cluster size during the collapse. The crossover point in the decay of $P(c_{ij})$ as a function of c_{ij} is estimated from the discrete local slope as calculated by

$$\gamma_t(c_{ij}) = -\frac{\Delta \ln[P(c_{ij})]}{\Delta \ln[c_{ij}]}.$$
 (1)

In Figure 5c of the main text, we have shown the plot of $\gamma_t(c_{ij})$ as function of c_{ij} at five different times for (Gly)₂₀₀. Here, in Figures 4b and 5b we show the same for (Gly)₁₀₀ and (Gly)₁₅₀, respectively.